



## 저작자표시-비영리-변경금지 2.0 대한민국

이용자는 아래의 조건을 따르는 경우에 한하여 자유롭게

- 이 저작물을 복제, 배포, 전송, 전시, 공연 및 방송할 수 있습니다.

다음과 같은 조건을 따라야 합니다:



저작자표시. 귀하는 원저작자를 표시하여야 합니다.



비영리. 귀하는 이 저작물을 영리 목적으로 이용할 수 없습니다.



변경금지. 귀하는 이 저작물을 개작, 변형 또는 가공할 수 없습니다.

- 귀하는, 이 저작물의 재이용이나 배포의 경우, 이 저작물에 적용된 이용허락조건을 명확하게 나타내어야 합니다.
- 저작권자로부터 별도의 허가를 받으면 이러한 조건들은 적용되지 않습니다.

저작권법에 따른 이용자의 권리는 위의 내용에 의하여 영향을 받지 않습니다.

이것은 [이용허락규약\(Legal Code\)](#)을 이해하기 쉽게 요약한 것입니다.

[Disclaimer](#)

Master's Thesis

# Sodium biphenyl as an anolyte for enhancing stability and capacity of sodium metal anode

Hyein Yu

Department of Energy Engineering  
(Battery Science and Technology)

Graduate School of UNIST

2019

# Sodium biphenyl as an anolyte for enhancing stability and capacity of sodium metal anode

Hyein Yu

Department of Energy Engineering  
(Battery Science and Technology)

Graduate School of UNIST

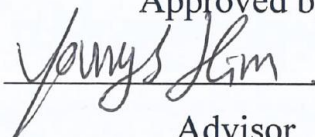
# Sodium biphenyl as an anolyte for enhancing stability and capacity of sodium metal anode

A thesis/dissertation  
submitted to the Graduate School of UNIST  
in partial fulfillment of the  
requirements for the degree of  
Master of Science

Hyein Yu

1. 10. 2019

Approved by



Advisor

Youngsik Kim

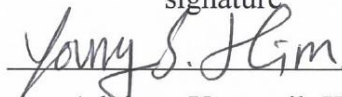
# Sodium biphenyl as an anolyte for enhancing stability and capacity of sodium metal anode

Hyein Yu

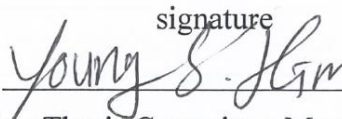
This certifies that the thesis/dissertation of Hyein Yu is approved.

1. 10. 2019

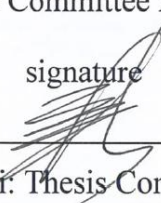
signature

  
Advisor: Youngsik Kim

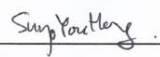
signature

  
Youngsik Kim: Thesis Committee Member #1

signature

  
Yun Seok Choi: Thesis Committee Member #2

signature

  
Sung You Hong: Thesis Committee Member #3

## Contents

Abstract .....	6
1. Introduction .....	7
1.1 Importance of Energy Storage System (ESS) .....	7
1.2 Previous researches of ESS .....	9
1.3 Seawater Battery (SWB) .....	10
1.3.1 Principles of SWB .....	10
1.3.2 Advantages and drawbacks of SWB .....	11
1.4 Research proposal .....	12
2. Results and Discussion .....	13
2.1 Sodium biphenyl (Na-BP) as a liquid anode .....	13
2.1.1 Anode properties .....	13
2.2 Sodium biphenyl (Na-BP) as a liquid electrolyte .....	17
2.2.1 Electrolyte properties .....	17
3. Experimental method .....	32
3.1 Fabrication method of Na-BP .....	32
3.2 Chemical composition .....	33
3.3 Optimization of cell components .....	35
4. Conclusion .....	36
5. References .....	37

## Abstract

Among various candidates of anode materials, Na metal anode which has the highest theoretical capacity and lowest redox potential is generally used for seawater battery. However, its high reactivity causes a lot of side reactions between electrode and electrolyte. Therefore, their severe decomposition is occurred and unstable solid electrolyte interphase (SEI) is formed. These drawbacks eventually induce volume expansion of cell by gaseous by-products and Na dendrite growth. Herein, we apply sodium biphenyl (Na-BP) as an electrolyte for its high stability with Na metal anode. Na-BP has both ionic and electronic conductivity as intrinsic properties. In that point, existing battery systems have hardly used Na-BP as an electrolyte.

Meanwhile, seawater battery is physically separated between cathode and anode with NASICON (Na Super Ionic Conductor) solid membrane. Using the closed-structure of anode, Na-BP can be applied in seawater battery without any concerns for internal short circuit. When Na-BP is used with Na metal anode, it can compensate capacity of Na metal anode with its intrinsic capacity. As an anolyte, it shows high capacity retention (91.8%) for 80 cycles in Na-BP // Seawater full-cell. Also, it does not contain decomposition reaction and SEI layer. As a result, Na-BP can suppress gas evolution and dendrite growth forming homogeneous surface of electrode. Moreover, Na-BP is about 13 times cheaper than conventional Na-salt-based electrolytes. It suggests potential application of seawater battery as one of the large-scale ESS.

## 1. Introduction

### 1.1 Importance of Energy Storage System (ESS)

Increasing demand of fossil fuels and coals causes serious problems of depletion of their resources and environmental pollution. So that it has been important to utilize renewable energy sources for the alternatives as days go by which use unlimited and eco-friendly energy sources. At the same time, the development and supply of energy storage systems (ESS) especially, large-scale ESS for storing electric energy produced from renewable energy sources such as wind, solar, and geothermal power as shown in Fig. 1a are becoming urgent for their continuously increased world energy consumption according to Fig. 1b. ESS can store and transmit electricity from the renewable energy sources. Moreover, it can supply electricity considering peak time for daily usage of electricity so that cost-efficient and stable supply can be possible.

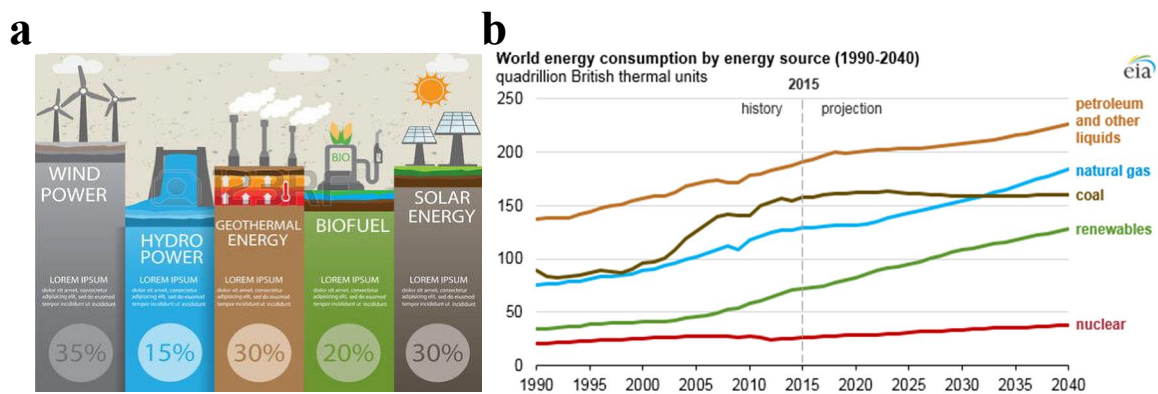


**Figure 1.** Importance and growth in demand of renewable energy sources as alternative to fossil fuels and coals; (a) Illustration and proportion of each kinds of renewable energy sources, (b) World energy consumption by energy source (1990-2040) (Energy Information Administration, EIA, U.S.) <sup>1</sup>.

Fig. 2 indicates total energy storage on the grid (ESG) world markets otherwise known as long-duration and large-scale ESS from 2012 until 2022 years. According to the chart, installed capacity of ESG has been steeply increased all over the world. To cover the expected demand and importance of ESS, researches and technical development for ESS should be actively supported.



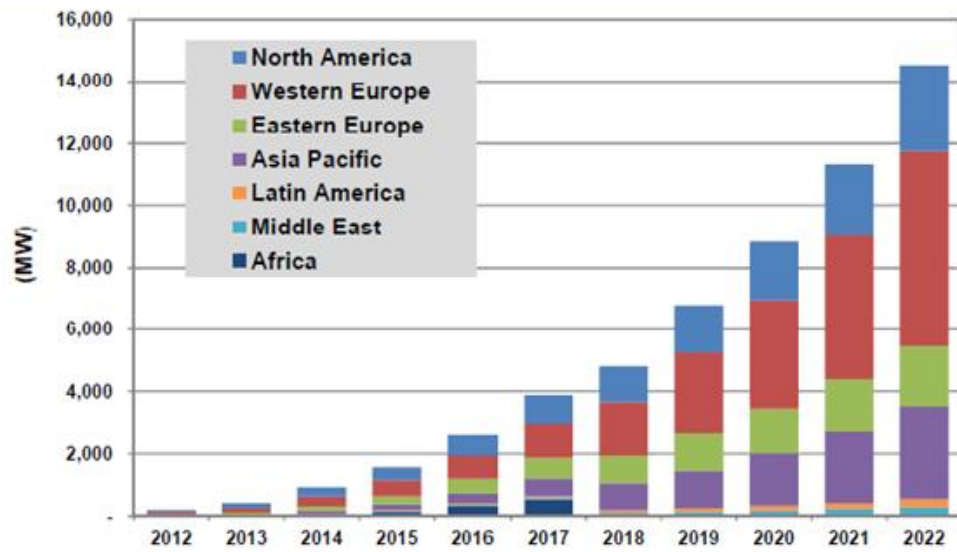


**Figure 2.** Total energy storage on grid (ESG) market, Installed capacity by region, World markets: 2012-2022 (Unit: MW, Source: Pike Research) <sup>2</sup>.

## 1.2 Previous researches of ESS

Among various candidates for energy storage system (ESS), batteries are the most widely used for storing electric energy based on reversible oxidation/reduction reactions with easily scalable advantages from small to large-scale ESS (Fig. 3a). Each battery systems are categorized by kinds of electro-active materials and characteristics of negative and positive electrode materials. Through this materials, main properties of the battery systems such as power density and energy density could be determined (Fig. 3b).

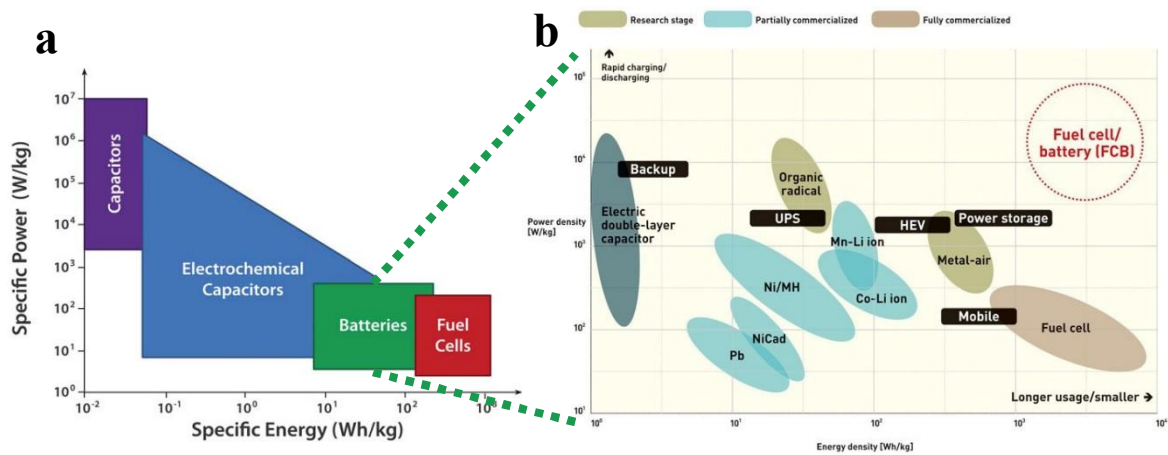


**Figure 3.** (a) Specific power as a function of specific energy for various energy storage devices, (b) Ragone plot comparing the performance of various batteries (Energy density vs. output density)<sup>3, 4</sup>.

Cobalt- and nickel-based cathode materials have been commonly used as the electrochemically used as one of the most stable cathode materials. However, they occupy over 35% of total cost in the most commercialized energy storage devices, lithium-ion batteries. Though cobalt and nickel are the key elements for these cathode materials, nickel is not only toxic but also cobalt has a limited global reserves and contributes to the rising prices every year of cathode materials and lithium-ion batteries due to unstable supply.

## 1.3 Seawater Battery (SWB)

### 1.3.1 Principles of SWB

In this regard, our group devised a new type of electric energy storage system called seawater battery (SWB). The seawater battery is operated by using seawater as an unlimited and eco-friendly resource as cathode material and produces and stores electricity through charge and discharge of sodium (Na) infinitely existing in seawater. Seawater, which functions as an aqueous electrolyte including abundant sodium ions, is catholyte in the SWB and it is physically separated to anode materials with Na Super Ionic Conductor (NASICON) solid electrolyte. This Na-ion conducting ceramic, NASICON, can selectively conduct sodium ions between seawater cathode and anode part with hopping mechanism<sup>5</sup>. The anode part of the SWB is composed by electro-active materials for Na-ion storage and non-aqueous electrolyte for Na-ion conduction. In that point, SWB contains three electrolytes that aqueous electrolyte-seawater catholyte, solid electrolyte-NASICON and non-aqueous electrolyte-organic liquid electrolyte<sup>6</sup>.

Fig. 4 indicates schematic illustration of SWB during charge process. During charge process, both oxygen evolution reaction (OER) with the theoretical cell voltage ( $E_{\text{cell}}$ ) as 3.48 V and chlorine evolution reaction (CER) are occurred with  $E_{\text{cell}}$  as 4.07 V at pH 8 condition. During discharge process, each opposite reactions, oxygen reduction reaction (ORR) and chlorine reduction reaction (CRR), are occurred as shown in below reaction mechanism in Fig. 4<sup>6,7</sup>.

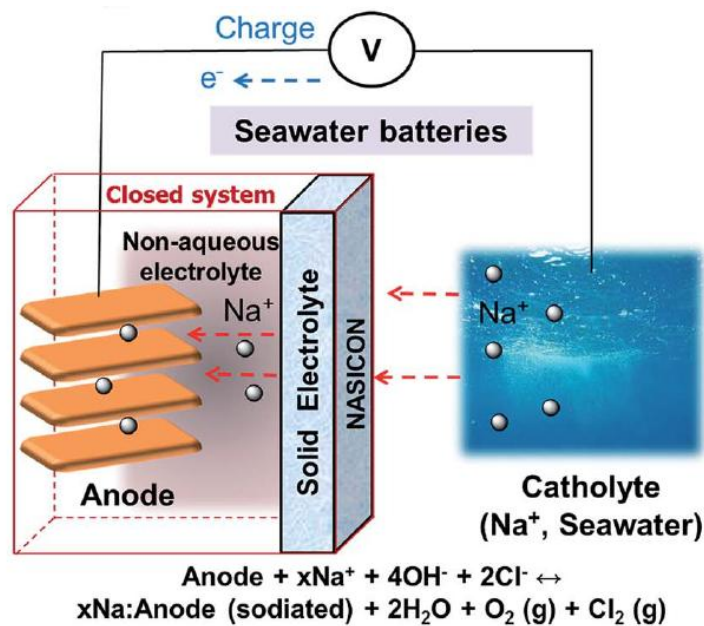


**Figure 4.** Schematic illustrations of seawater batteries and charge-discharge mechanism in seawater batteries<sup>6</sup>.

### 1.3.2 Advantages and drawbacks of SWB

This eco-friendly rechargeable battery can prevent cost and supply concerns of conventional battery systems. Furthermore, the open-structure of seawater cathode can have high energy density and the seawater cathode does not limit capacity so that the capacity of the seawater battery is only determined by anode. Among the anode active material candidates, sodium (Na) metal anode which is easy to access and has low price is mainly used by the sixth most abundant element in the earth, Na. Na metal anode has low oxidation and reduction potential and high capacity ( $1156 \text{ mAh g}^{-1}$ ). The cathode and anode of the cell are separated by a solid electrolyte, NASICON (Na Super Ionic Conductor) membrane. As a result, the seawater battery has a structure in which the cathode and the anode are physically separated.

In spite of various advantages mentioned above, Na metal anode is an alkali metal which has tremendous reactivity. During charging and discharging process, it generates various organic gases including hydrogen gas in consequence of serious decomposition reaction with organic electrolyte in anode<sup>8</sup>. Thereby, unstable solid electrolyte interphase (SEI) layer is formed between anode and electrolytes. This causes serious safety problems and cell failure due to the formation of explosive gases during decomposition reactions and SEI formation. Also, unstable and heterogeneous surface induce locally enhanced electric field or different ion diffusion rate. It makes sodium dendrite growth and the initially formed dendrite accelerates further dendrite growth<sup>9, 10</sup>. This dendrite growth causes serious safety problems such as internal short circuit and cell explosion. Moreover, electrolyte depletion and anode capacity fading with low reversibility are happened and these degrade cell performance critically<sup>11</sup>.

## 1.4 Research proposal

Herein, sodium biphenyl (Na-BP) is studied in this research as an anolyte in SWB, which has been used as a liquid anode material or chemical sodiation agent for electrodes in conventional energy storage devices <sup>12, 13</sup>. As a liquid electrolyte, Na-BP can conduct Na-ions and has high stability with Na metal anode. And simultaneously as a liquid anode, Na-BP can compensate the capacity of Na metal anode.

Na-BP has both intrinsic electric and ionic conductivity, so it was difficult to be applied as an electrolyte in the conventional battery system because of internal short circuit where electrons are passed through the cathode and anode <sup>14</sup>. However, seawater battery which can selectively pass sodium ions with NASICON membrane can apply Na-BP as one of the next-generated electrolytes without any concerns of internal short circuit.

When Na-BP is prepared, Na metal is applied to saturated concentration by adding excessive Na metal into biphenyl-ether solution. In that point, Na-BP can be used as highly stable electrolyte without reactivity with Na metal anode.

When Na-BP is applied as an anolyte, it is confirmed that Na-BP has a theoretical capacity of  $29.3 \text{ AhL}^{-1}$  as liquid anode and can compensate capacity of anode with high coulombic efficiency of 95% over 80 cycles in Na-BP // seawater full-cell.

In addition, as a liquid electrolyte, there is no reactivity with Na metal anode to suppress evolution of gas byproducts, thereby preventing the expansion of the battery and solving the limitation of the conventional liquid electrolyte. Also, due to its less reactivity with anode, when sodium is plated during charging, stable electrolyte-electrode interfaces are formed and it can suppresses dendrite growth with high overpotential decreasing nucleation rate during metal plating <sup>15</sup>.

Moreover, existing sodium salt-based electrolytes have high cost, while Na-BP is about 13 times much cheaper than them. These results indicate that Na metal anode can potentially be applied to large-scale ESS and seawater battery is enough to become a candidate of large-scale ESS.

## 2. Results and Discussion

### 2.1. Sodium biphenyl (Na-BP) as a liquid anode

#### 2.1.1 Anode properties

When conventional sodium or lithium salt-based electrolyte is prepared, generally white salts are dissolved into organic solvent and the electrolyte seems like transparent solution. However, when specific aromatic hydrocarbon compounds such as biphenyl or naphthalene are dissolved in an ether-based solvent, an alkali metal such as lithium and sodium metal can be dissolved into the solution and it undergoes charge transfer reaction<sup>16, 17</sup>. As a results, alkali-biphenyl or alkali-naphthalene solutions have dark blue color like Fig. 5.

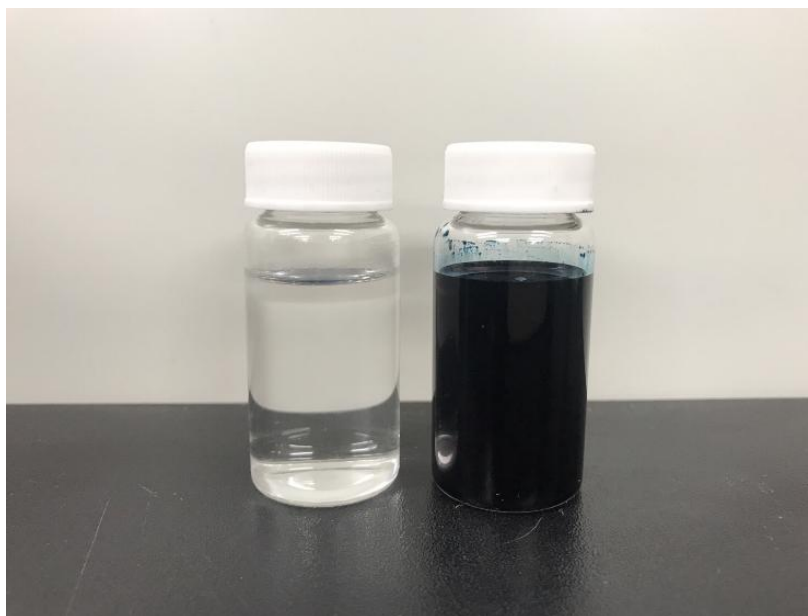


**Figure 5.** Photograph of 1 M sodium triflate-TEGDME (Left) and saturated sodium-1 M biphenyl-DEGDME in transparent vial (Right).

One of the alkali-biphenyl solutions, sodium biphenyl (Na-BP) solution, is fabricated by sodium metal as an alkali metal, biphenyl and diethylene glycol dimethyl ether (DEGDME) solvent in this research. This Na-BP has been widely used as liquid anode in various battery systems<sup>12, 18</sup>. In that point, when Na-BP is applied as an anolyte in seawater battery (SWB), it can have anode properties in SWB as well. If anode half-cell tests are done with general structure of half-cell, there must be internal short circuit (ISC). So new structure shown in Fig. 6 of anode half-cell using 2046 coin-type cell is constructed to confirm intrinsic properties of Na-BP as a liquid anode. Solid electrolyte, NASICON which can selectively pass Na-ions, is applied as membrane for preventing ISC between sodium metal and liquid anode, Na-BP.

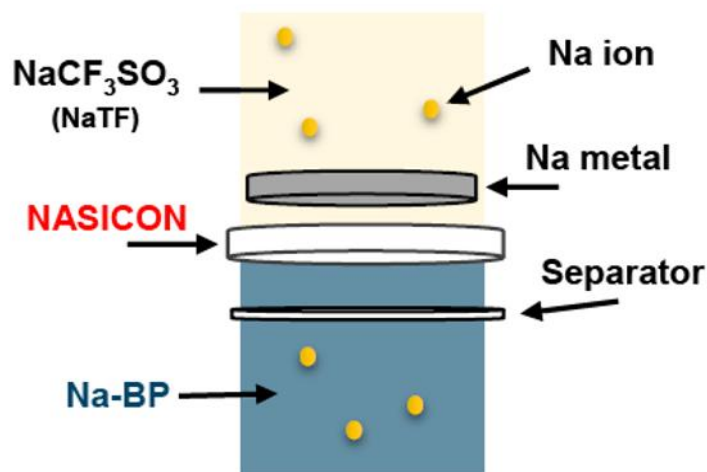


**Figure 6.** Illustration of Sat. Na-1 M BP-DEGDME half-cell structure and components.

Fig. 7a indicates the sodiation and desodiation voltage profiles during the initial 1st and 2nd cycle of Na/Na-BP anode half-cell at a current density of  $0.5 \text{ mA cm}^{-2}$ . Sodiation voltage plateau is around 0.1 V and desodiation voltage plateau is around 0.3 V versus Na/Na<sup>+</sup>. Through ICP analysis, saturated concentration of sodium in Na-BP is measured about 1.1 M and theoretical capacity is calculated as  $31.2 \text{ mAh g}^{-1}$ . Actual initial discharge capacity of Na-BP was as low as  $15.7 \text{ mAh g}^{-1}$ , but this was attributed to the loss due to cell assembly process and wetting with both the NASICON and separator since the anode itself was in a liquid state. However, Na-BP shows 79.6% capacity retention based on irreversible reaction of the initial cycle, and stable cycle performance with high coulombic efficiency of 99.8% during 80 cycles as seen in Fig. 7b.

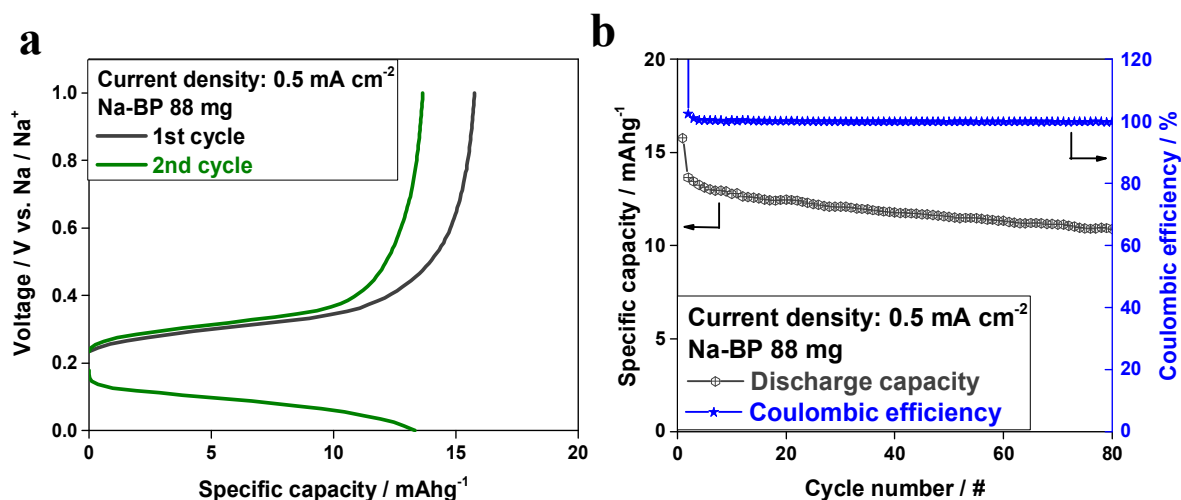


**Figure 7.** Anode properties of Na-BP-DEGDME liquid solution; (a and b) Cycle performance of Na-BP-DEGDME liquid anode half-cell; (a) Charge-discharge voltage profiles at a current density of  $0.5 \text{ mA cm}^{-2}$ , (b) cycle ability of Na-BP-DEGDME liquid anode half-cell.

Also, further electrochemical test was done in Na-BP//Seawater full-cell with 2046 coin-type seawater battery as shown in Fig. 8a<sup>6</sup> and nickel foam is used for current collector in Na-BP anode part. Fig. 8b shows discharge-charge voltage profiles of constructed Na-BP//Seawater full-cell during 1st and 2nd cycle at a current density of  $0.5 \text{ mA cm}^{-2}$  in seawater battery. In the full-cell, Na-BP maintains 94.2% of the capacity after 80 cycles on the basis of initial discharge capacity  $20.5 \text{ mAh g}^{-1}$  and exhibits high coulombic efficiency of 92.7% (Fig. 8c). These results show Na-BP can compensate capacity of seawater battery for its reliable intrinsic capacity with low capacity decay when it is applied as a liquid electrolyte in seawater batteries.



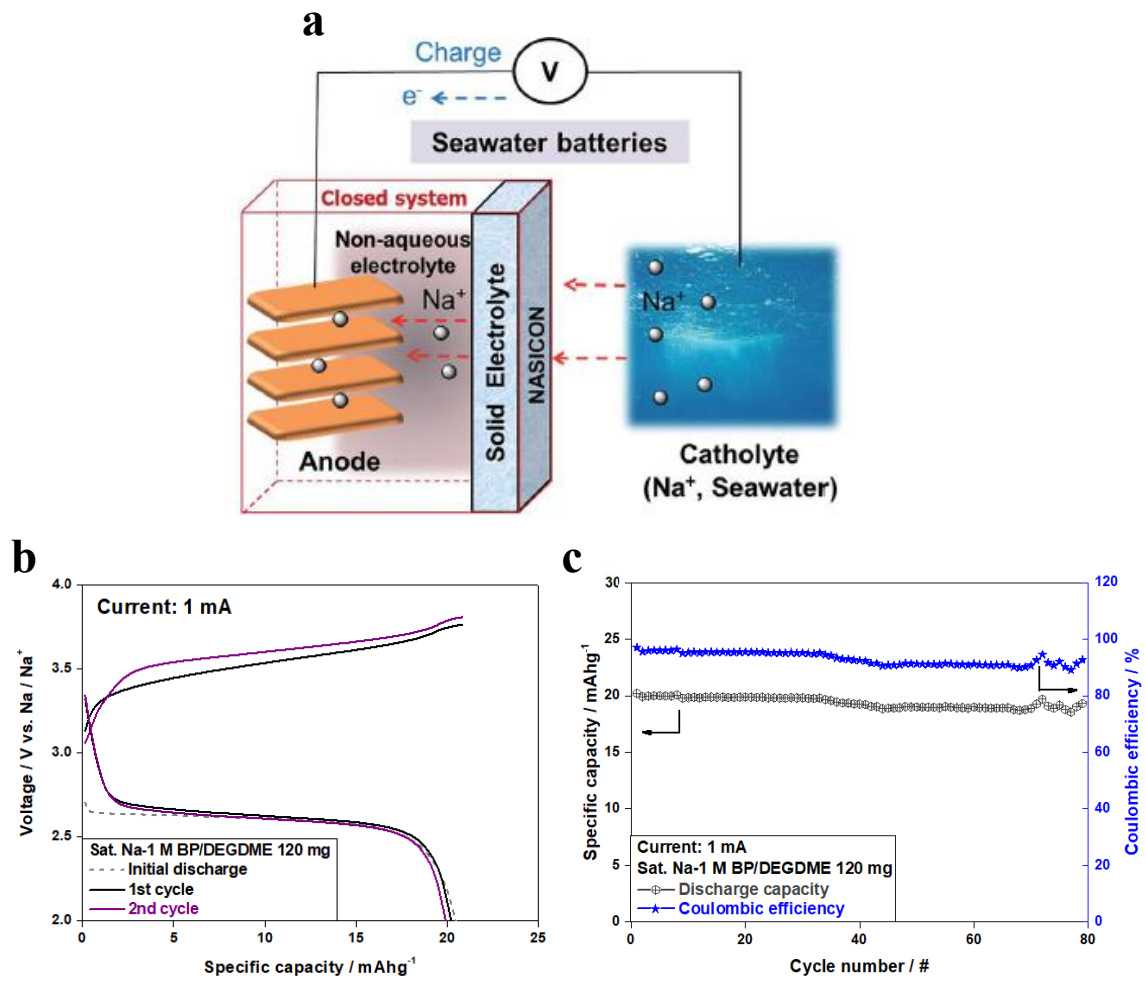


**Figure 8.** Electrochemical properties of Na-BP-DEGDME anode // seawater full-cell with seawater-flow type cell; (a) Illustration of Sat. Na-1 M BP-DEGDME // seawater full-cell structure and components <sup>6</sup>, (b and c) Cycle performance of Na-BP-DEGDME full-cell at a current density of 0.5 mA cm<sup>-2</sup>; (b) charge-discharge voltage profiles, (c) cycle ability of Na-BP-DEGDME // seawater full-cell at a current density of 0.5 mA cm<sup>-2</sup>.

## 2.2. Sodium biphenyl (Na-BP) as a liquid electrolyte

### 2.2.1 Electrolyte properties

When Na-BP was substituted for existing organic electrolytes, we designed an experiment to verify the most important property as an electrolyte, which is ionic conductivity. The measured conductivity value of Na-BP using conductivity meter is  $7.06 \times 10^{-3} \text{ S cm}^{-1}$ , which indicates total conductivity of Na-BP including ionic and electronic conductivity. The isothermal transient ionic current (ITIC) method was used to separate the total conductivity and confirm the ionic conductivity of Na-BP at room temperature <sup>19</sup>. Using 2032 coin cell, the cell for measuring conductivity of NA-BP by ITIC method was constructed as shown in Fig. 9. Two stainless steel electrodes are separated with glass fiber separator which is immersed with Na-BP.

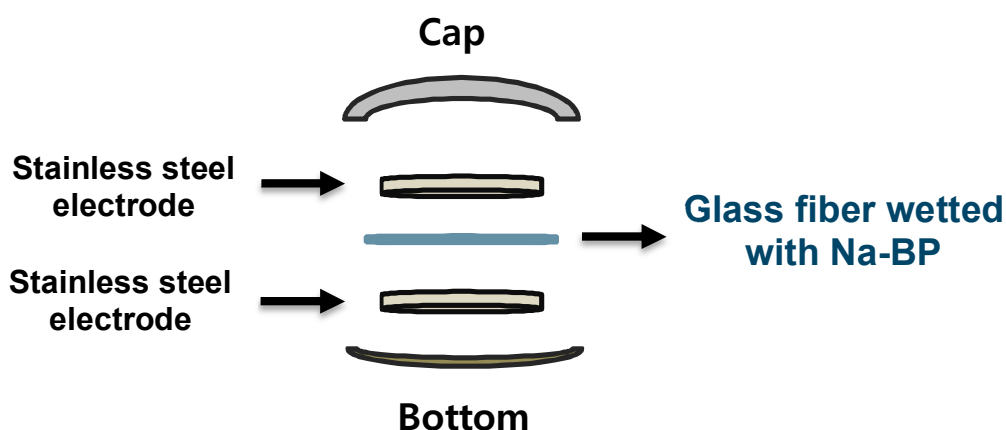


**Figure 9.** Cell design for conductivity measurement of Na-BP-DEGDME anolyte with isothermal transient ionic current (ITIC) method.

When 0.1 V is applied as an initial potential to the cell at the room temperature (25 °C), the graph of current versus time is obtained as shown in Fig. 10. The region of graph that current is rapidly dropped from about 8.6 mA to 6.2 mA is due to existence of ionic transport by Na-BP. Also, electronic conductivity of Na-BP always exists in all current region in the graph <sup>20</sup>.

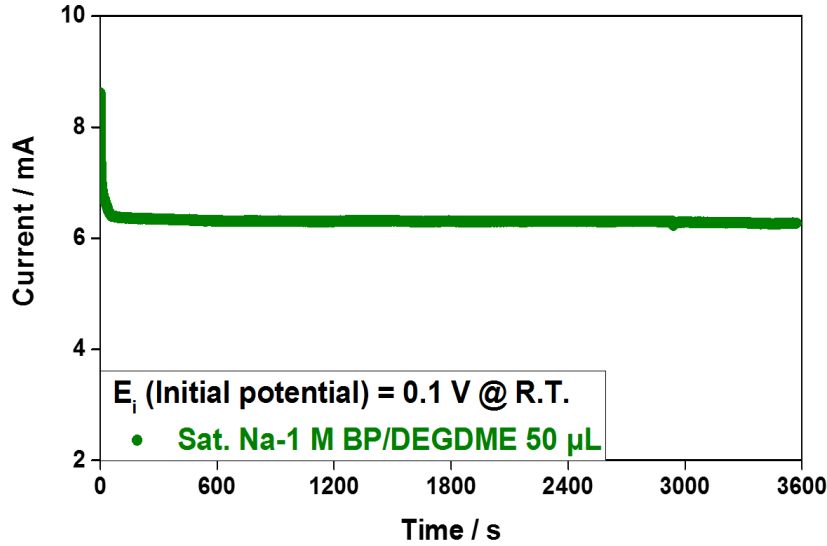


**Figure 10.** Measured ionic and electronic conductivity from ITIC (Isothermal transient ionic current) method.

When the graph is fitted to below equation, the calculated ionic conductivity of Na-BP is  $9.4 \times 10^{-4} \text{ S cm}^{-1}$  and electronic conductivity is  $1.5 \times 10^{-3} \text{ S cm}^{-1}$ .  $J$  is the current density over time,  $\sigma_{dc,e^-}$  indicates the electronic conductivity,  $\sigma_{dc,Na^+}$  indicates the ionic conductivity,  $U$  is the applied voltage between two electrodes,  $\mu_{Na^+}$  is the sodium ion mobility and  $t$  is the time <sup>20</sup>.

$$J(t) = \frac{\sigma_{dc,e^-} U}{L} + \frac{\sigma_{dc,Na^+} U}{L} \exp\left(-\frac{\mu_{Na^+} U}{L^2} t\right)$$

Generally, the sum of the ionic conductivity and the electronic conductivity is regarded as the total conductivity. The calculated total conductivity is obtained by combining the above two values was  $2.44 \times 10^{-3} \text{ S cm}^{-1}$ , which is twice as low as the total conductivity measured by the conductivity meter. The exact value of ion conductivity of Na-BP is expected to be higher considering the error of the conductivity measured by ITIC analysis method.

Further experiments are designed to check whether Na-BP could plate and strip sodium ions to the anode side as an electrolyte beyond its own capacity. An anode half-cell test with a carbon felt (CNF) as an anode current collector with Na-BP as an electrolyte and CNF | Na-BP | Seawater full-cell test was performed.

Through the CNF anode current collector half-cell test with Na-BP anolyte, voltage profile was obtained (Fig. 11a). There are mainly 3 steps during the test. Above all, desodiation for intrinsic capacity of Na-BP is done under 1 V cut-off condition at the current density of  $0.25 \text{ mA cm}^{-2}$  was performed.

After the desodiation step, Na-BP is sodiated as 2.8 mAh of the confirmed capacity previous step and Na plating is done approximately as 0.7 mAh, corresponding to about 25% of the sodiation capacity.

In the next step, Na stripping and a Na-BP desodiation process were performed under 1 V cut-off condition. As shown in Fig. 11a, distinct voltage plateau region of Na plating around -0.05 V was observed along with voltage plateau region of the sodiation process of Na-BP around 0.1 V. And voltage plateau region of Na stripping around 0.05 V and voltage plateau region of the desodiation process of Na-BP was confirmed around 0.25 V as well. As a result, it was found that the Na-BP could plating and stripping Na ions sufficiently beyond its own capacity.

Moreover, when the intrinsic capacity of Na-BP was completely discharged in Na-BP // seawater full-cell at initial step, the observed discharge capacity of Na-BP is as 2.5 mAh in Fig. 11b.

After charging as 2.5 mAh, an additional 1.5 mAh capacity was plated and 1 V cut-off discharge step was conducted and the cycling was done with these steps. As a result, it exhibited a high coulombic efficiency of more than 92% with stable voltage profiles.

From the results in Fig. 11a and 11b, Na-BP can conduct Na ions enough as an electrolyte so that reliable Na plating and stripping is possible over its own capacity in seawater battery system as well.

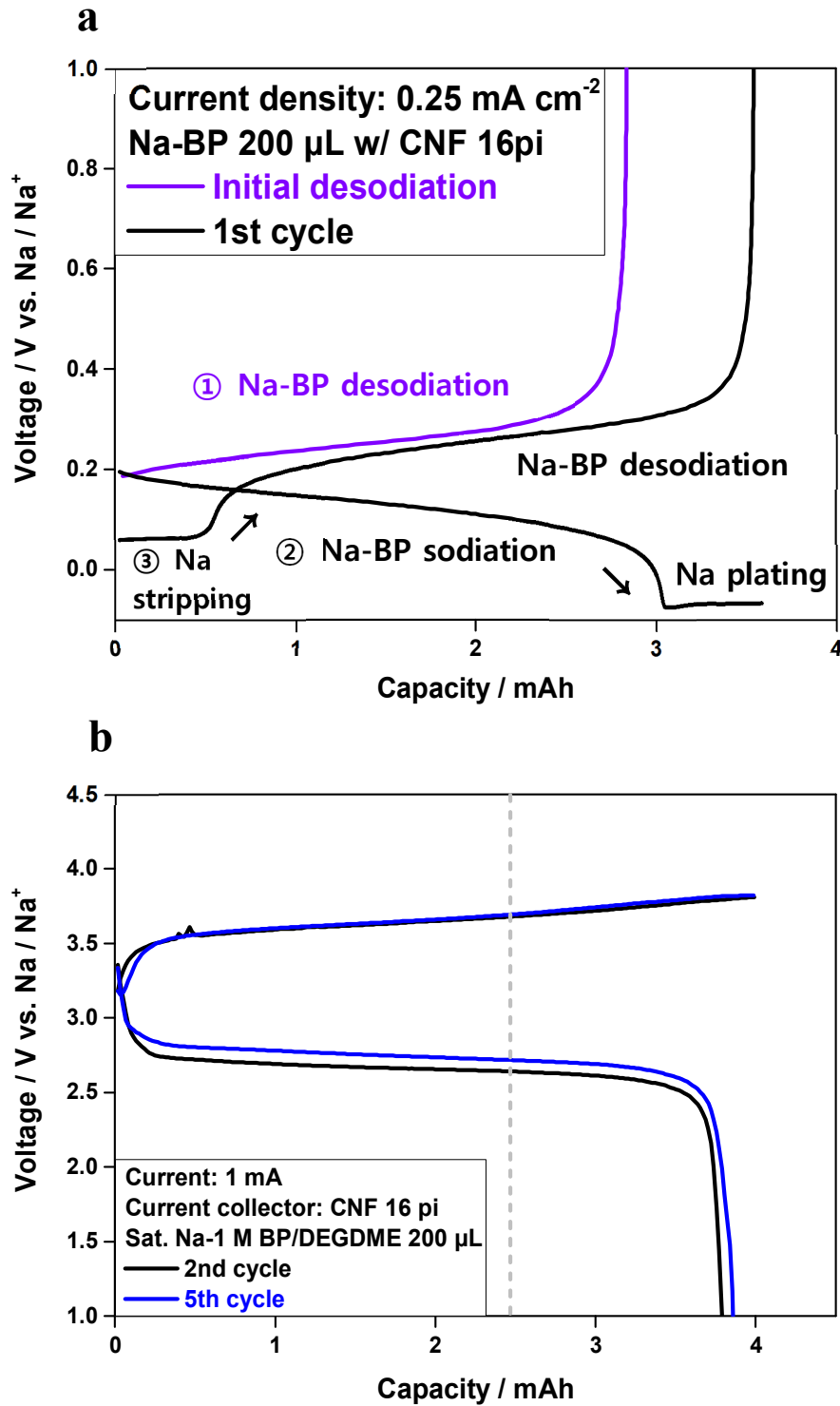


**Figure 11.** Electrolyte properties of Na-BP-DEGDME; (a and b) Na plating/stripping performance with Na-BP-DEGDME analytes; (a) in anode half-cell at a current density of  $0.25 \text{ mA cm}^{-2}$ , (b) in current collector | seawater full-cell at a current density of  $0.5 \text{ mA cm}^{-2}$ .

Next, I verified whether Na-BP was used as an electrolyte in seawater battery to inhibit decomposition reaction due to stability with Na metal anode and to suppress gas by-products through DEMS gas analysis.

Cylindrical DEMS cell is constructed like Fig. 12. The cell contains seawater cathode, NASICON solid membrane, electrolytes and Na metal anode having the same structure as that of seawater battery. DEMS analysis can detect the gas species and the amount of gas generated by analyzing the molecular weight of gas generated during charging and discharging process of DEMS cell by injecting Ar gas as a carrier gas.

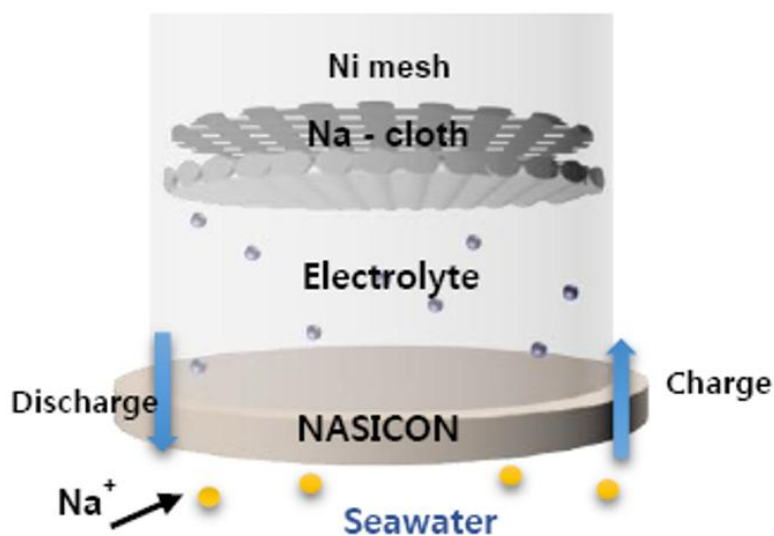


**Figure 12.** Schematic illustration of DEMS cell for analyzing evolved gas during charge-discharge cycling.

In this experiment, the gas generated during charging and discharging process was confirmed applying Na-BP-DEGDME and NaTF-TEGDME electrolyte, respectively. At the current density of  $0.25 \text{ mA cm}^{-2}$ , charging and discharging cycling for 10 hours is done like Fig. 13a and 13b. It is confirmed that negligible amount of gas is generated when applying Na-BP electrolyte through result in Fig. 13c. Also, when Na-BP is applied as an anolyte, it indicates relatively stable voltage profiles with lower overpotential. However, conventional electrolyte (NaTF-TEGDME) causes a severe decomposition reaction with Na metal with relatively unstable voltage profiles and overpotential in the same condition as shown in Fig. 13b. According to Fig. 13d,  $\text{H}_2$  gas as a major gas by-product is observed to be generated during the cycling with conventional electrolyte.

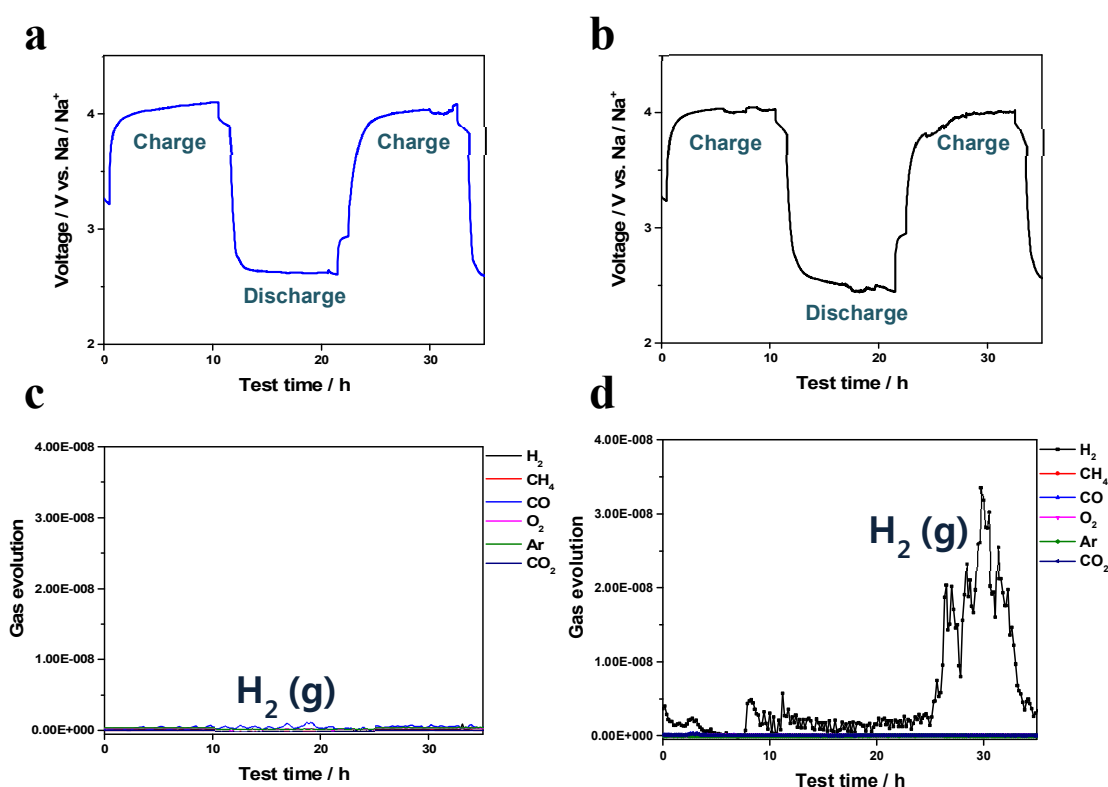


**Figure 13.** Gas evolution by electrode-electrolyte interaction in operating seawater cell; (a and b) Galvanostatic charge-discharge voltage profiles of (a) Na metal | Na-BP-DEGDME | Seawater DEMS cell, (b) Na metal | NaTF-TEGDME | Seawater DEMS cell (c and d) In-situ DEMS result data.

This cell expansion problems are remarkably observed in pouch-typed cells because of their possibility of cell swelling. When a current density of  $0.25 \text{ mA cm}^{-2}$  10 h condition was applied to cycling in each of the seawater pouch cells causing serious cell expansion problems were occurred due to the generation of gas by-products.

As shown in Fig. 14, it was confirmed that the existing electrolyte had only cycle life as 17 cycles with a high overpotential. However, in case of Na-BP electrolyte, the cell maintained over 30 cycles with stable cycle performance and low overpotential having high stability with Na metal anode. In addition, the Na-BP does not form SEI layer (Solid electrolyte interphase) with Na metal anode due to its electronic conductivity as well as its low reactivity with the anode and inhibits the decomposition reaction that forms the unstable SEI layer.

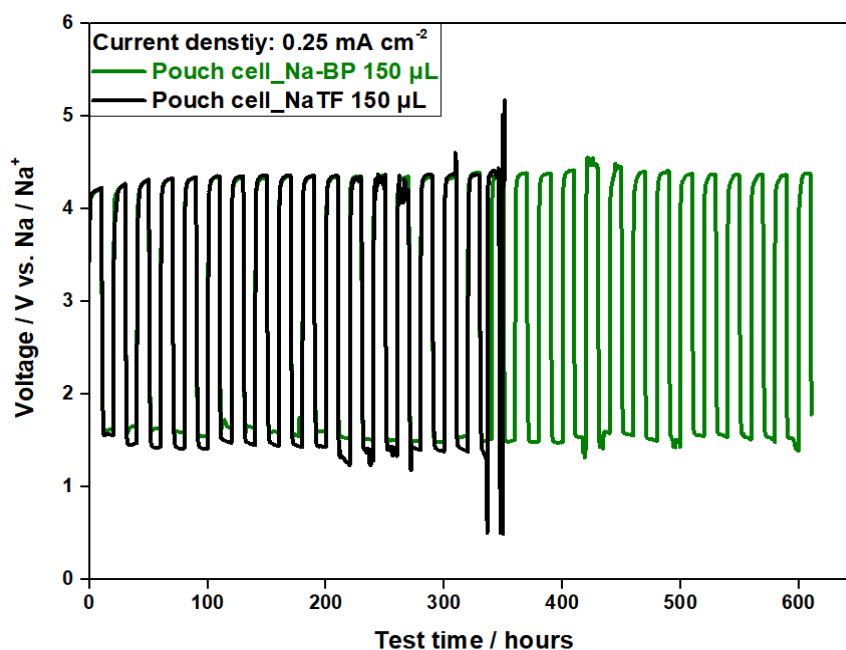
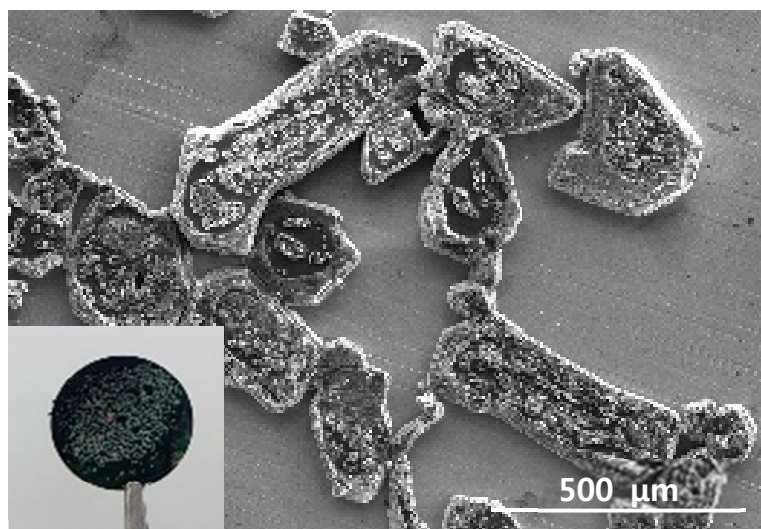


**Figure 14.** Cycle performance of Na metal | Na-BP-DEGDME and NaTF-TEGDME respectively | Seawater pouch-type cathode half-cell at a current density of  $0.25 \text{ mA cm}^{-2}$



Further experiments were carried out in which Na ions are plated to the copper (Cu) foil at the anode through seawater cathode. After plating test, remained electrolytes were removed by washing with 1,2-dimethoxyethane (DME) solvent. SEM images of each surface of foils are indicated in Fig. 15a and 15b. In the case of applying Na-BP electrolyte, the plated Na grain was much larger than that of NaTF electrolyte. The surface with larger grain could contain much homogenous surface as well.

**a**



**b**

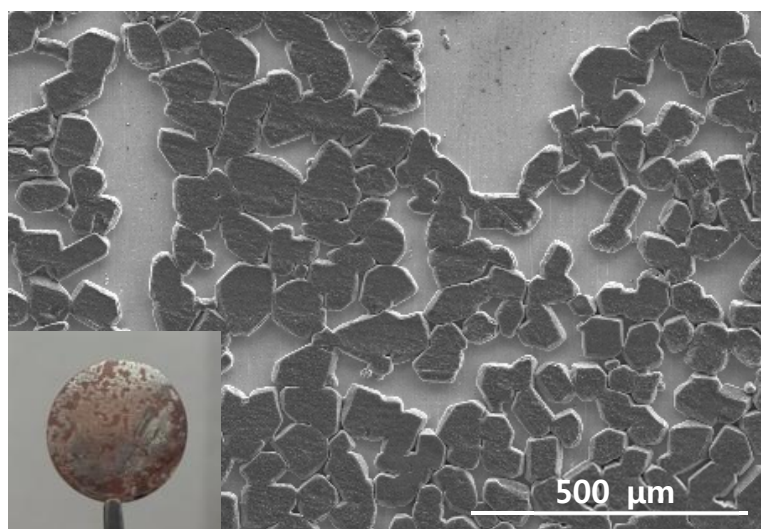


**Figure 15.** Photographs and SEM images of plated Na metal in seawater coin cell at a current density of  $0.1 \text{ mA cm}^{-2}$  with (a) Na-BP-DEGDME (b) NaTF-TEGDME anolyte.

These plated sodium grains and Cu foils were confirmed by EDS-mapping analysis which can distinct various elements on SEM images. According to the Fig. 16a and 16b, most of the plated islands are consisted of sodium. The region except these islands are composed of copper elements (Fig. 16c and 16d)<sup>21</sup>.

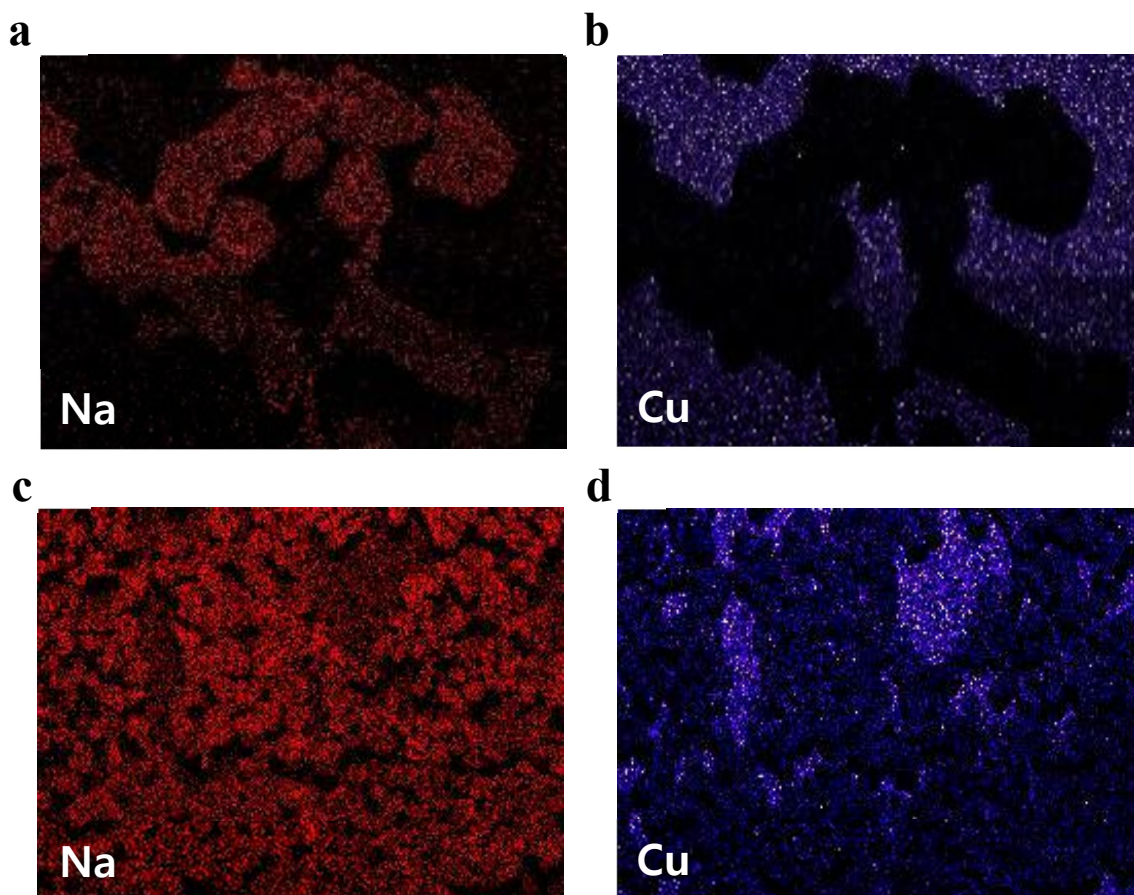


**Figure 16.** EDS-mapping results of plated Na metal in seawater coin cell at a current density of  $0.1 \text{ mA cm}^{-2}$  (a and c) Sodium (Na) elements, (b and d) Copper (Cu) elements with Na-BP-DEGDME and NaTF-TEGDME anolyte respectively.

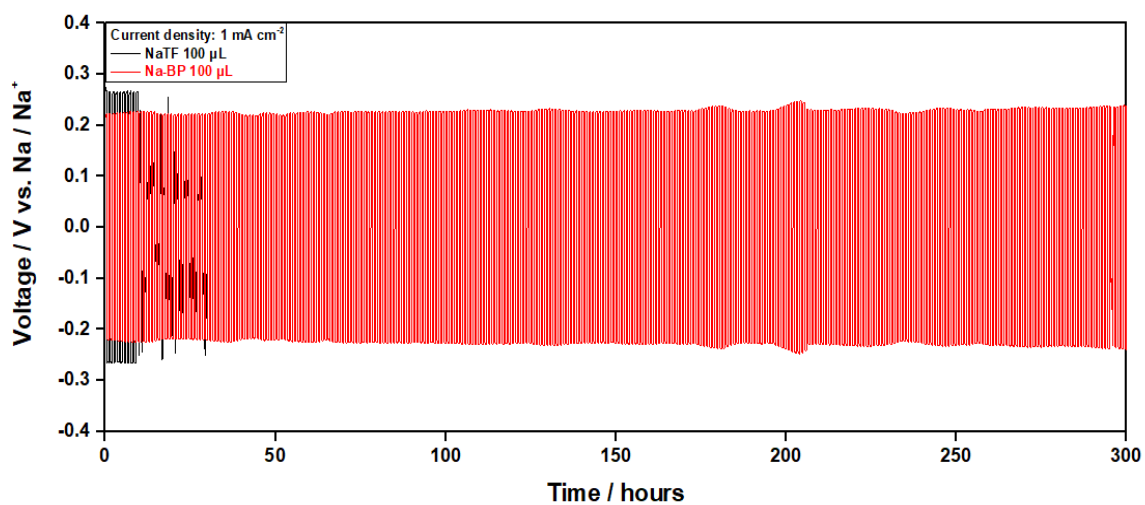
The heterogeneous interface created by the decomposition reaction between Na metal anode and electrolyte lowers the energy barrier forming Na nucleation. By the below equations, low energy barriers facilitate nucleation and lead to rapid nucleation rates, thereby promoting dendrite growth. In the equations,  $\Delta G^*$  represents energy barrier in nucleation,  $\gamma$  is interfacial energy between sodium and electrolyte,  $V_m$  is the molar volume,  $F$  is faraday's constant,  $\eta$  is nucleation overpotential at beginning of nucleation and  $r^*$  is critical radius of nucleation. By arranging the equations, energy barrier value is proportional to the square of critical radius of sodium nucleation and the interfacial energy between sodium and electrode<sup>22</sup>.

$$\Delta G^* = \frac{16\pi \gamma^3 V_m^2}{3 F^2 |\eta|^2} = \frac{4\pi}{3} (r^*)^2 \gamma$$

To confirm whether Na-BP shows more stable and lower overpotential than the existing electrolyte or not, Na-Na symmetric cells were fabricated and Na plating and stripping tests were done with these cells at current density of 1 mA cm<sup>-2</sup>. Like Fig. 17a, NaTF electrolyte exhibited overpotential as much as about 540 mV during 10 cycles, then cell showed unstable cycle performance within 30 cycles and internal short circuit (ISC) was occurred due to Na dendrite growth.

On the other hand, the cell with Na-BP electrolyte was operated stably while maintaining the overpotential about 440 mV during 300 cycles which was about 100 mW lower than NaTF. Furthermore, when the voltage profiles are enlarged in 20 – 30 hours region, the voltage profiles applied with conventional electrolyte shows much unstable cell operation than Na-BP case.

**a**



**b**

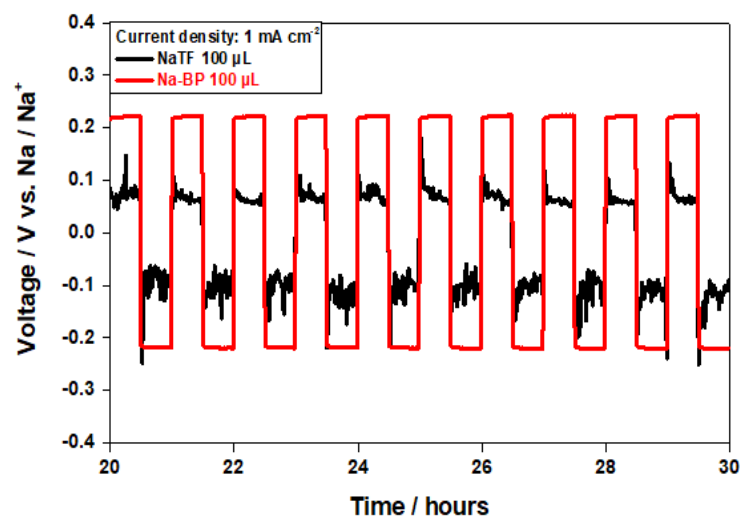


**Figure 17.** (a) Symmetric cell performance at a current density of 1 mA cm<sup>-2</sup> with Na-BP-DEGDME and NaTF-TEGDME electrolyte respectively, (b) Enlarged voltage profiles between 20 – 30 hours region.

In order to confirm the suppression of sodium dendrite growth in visual, the Swagelok cell made of transparent quartz is designed like Fig. 18.

After inside of the cell is filled with each electrolytes and current is applied, Na ions move from Na metal electrode on the top to bottom side and Na ions begin to be plated on the surface of bottom.

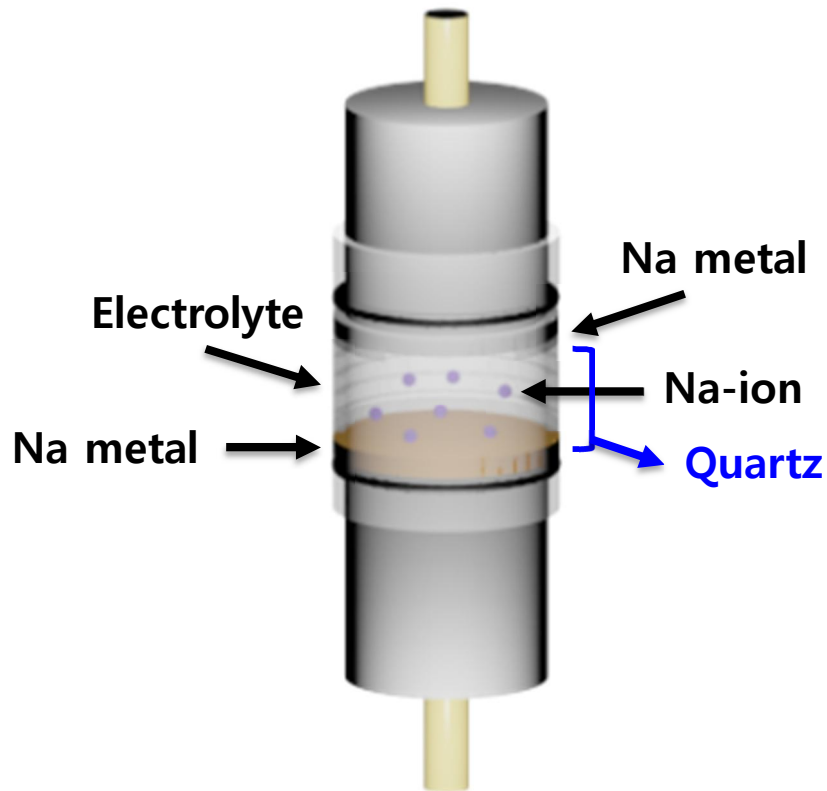


**Figure 18.** Schematic illustration of Swagelok cell design for confirming Na dendrite growth in visual.

When Na-BP electrolyte is applied with this test condition at a current density of about  $1.6 \text{ mA cm}^{-2}$ , Fig. 19a and 19b indicates each images of plated sodium at initial state and 250 minutes after the cell operation. As a result, the cell is operated until about 300 hours with extremely overpotential compared to conventional electrolyte, NaTF (Fig. 19c).

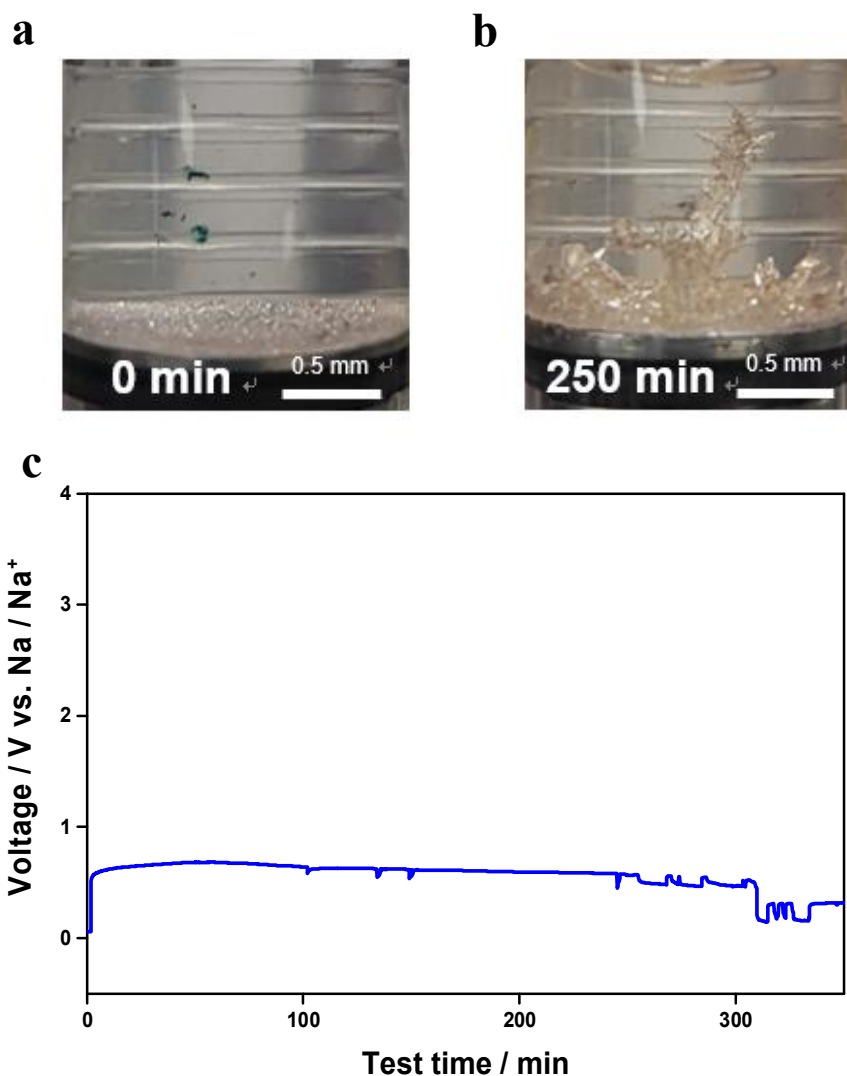
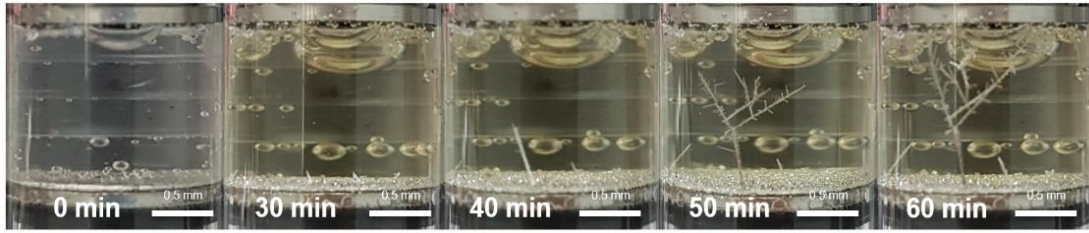


**Figure 19.** (a and b) Time-lapse images during Na dendrite growth on Na metal in Swagelok cell at a current of  $1.6 \text{ mA cm}^{-2}$  with Na-BP-DEGDME anolyte; (a) initial state (0 minute), (b) after 250 minutes passed state and (c) voltage profiles of the cell test.

Otherwise, when NaTF electrolyte is applied, it was confirmed that internal short circuit occurred in 60 minutes due to the sodium dendrite growth with the high overpotential more than 5 times in Na-BP case during the plating step in Fig. 20b. Likewise, time-lapsed images were taken according to the elapsed time of the plating step. The time-lapsed images in Fig. 20a shows that if NaTF electrolyte is used, sodium dendrite is formed like a very thin spindle due to rapid dendrite growth and localized accumulation of sodium in a specific region of the bottom <sup>23</sup>.

In other words, Na-BP can suppress the decomposition reaction when it is applied as an electrolyte and form more homogenous interface with the anode, so that the energy barrier to Na nucleation is high. Therefore, sodium grain is formed stably in Na-BP case with low overpotential during nucleation and retarded nucleation rates so actual dendrite growth can be delayed.

**a**



**b**

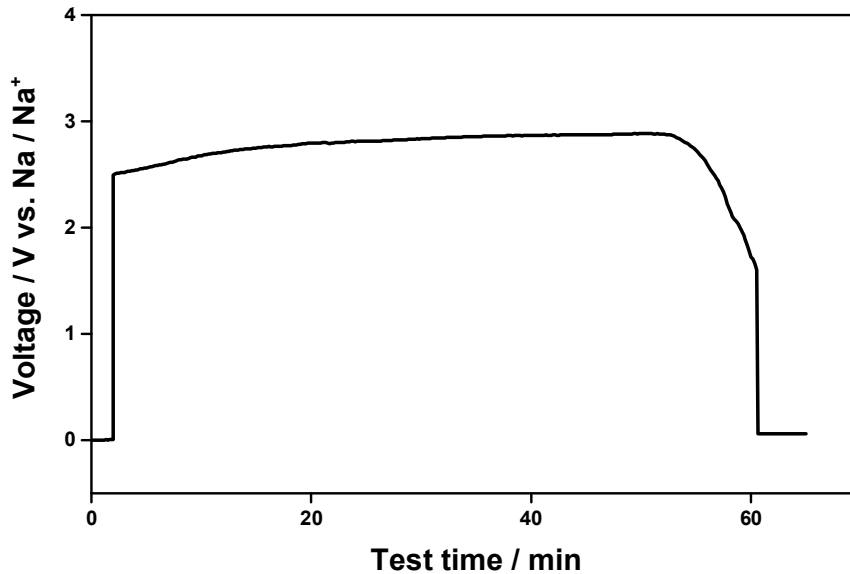


**Figure 20.** (a) Time-lapse images during Na dendrite growth on Na metal in Swagelok cell at a current of  $1.6 \text{ mA cm}^{-2}$  with NaTF-TEGDME anolyte from initial state (0 minute) to final state (after 60 minutes passed), (b) voltage profiles of the cell test.



Additional advantage of Na-BP as anolyte is cost aspect. Most of sodium-based salts for liquid electrolyte have highly expensive cost. However, Na-BP-DEGDME has about 13 times lower cost than typical electrolyte NaTF-TEGDME (Fig. 21). In this research, chemical composition of Na-BP is saturated Na and 1 M biphenyl in DEGDME. Total amount of Na metal is used as much as 1.5 M. Actually, cost of DEGDME and TEGDME per liter has negligible difference. Main difference is determined by cost of the salt. In Na-BP, cost of Na and biphenyl occupies only 18.7% of the total cost. Otherwise, cost of NaTF salt occupies 91.6 % of the total cost in NaTF electrolyte. This advantage of Na-BP in cost aspects can suggest not only potential application of Na-BP as stable anolyte for Na metal anode but also seawater battery as one of the large-scale ESS.

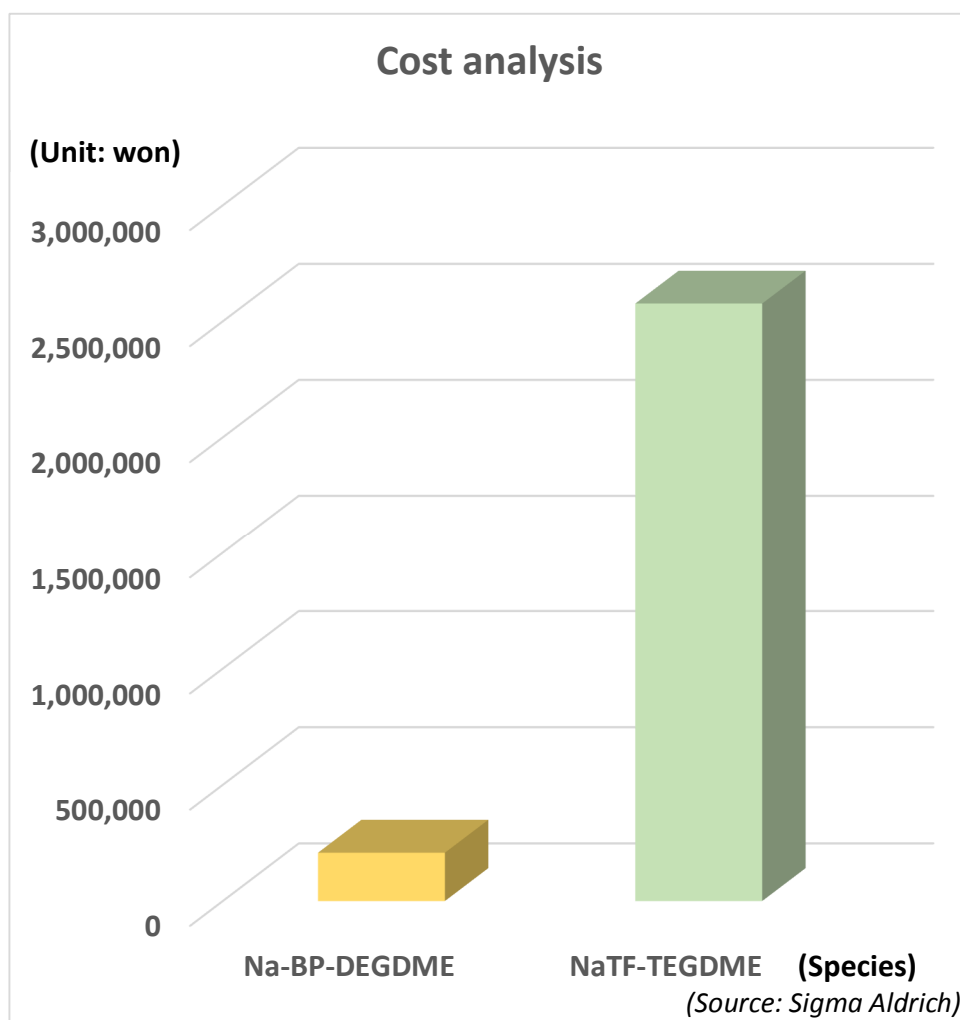


**Figure 21.** Cost comparison of Sat. Na-1 M BP in DEGDME and 1 M NaTF in TEGDME (Conventional electrolyte), (Source: Sigma Aldrich)



### 3. Experimental method

#### 3.1. Fabrication method of Na-BP

For the anolyte, sodium biphenyl solution was prepared by roughly 3 steps as shown in Fig. 22. One of glyme-based solvent diethylene glycol dimethyl ether (DEGDME) which has synonym as Bis(2-methoxyethyl) ether (Sigma Aldrich, 99%) was water-refined by molecular sieves (Samchun chemical, 4A 8-12mesh) for 1 day. Then, firstly 1 M biphenyl (BP) salts (Sigma Aldrich, 99.5%) were added into the refined DEGDME solvent. This biphenyl-DEGDME solution was stirred over 10 hours. After the complete stirring, 1 M sodium (Na) metals (Sigma Aldrich, 99.5%) and additional DEGDME solvents were added into the solution as second step. Total concentration of the solution is 1 M concentration with each biphenyl and Na metal. This step includes charge transfer reaction and then alkali metal-biphenyl-ether solution is fabricated. As a final step, excessive Na metals approximately 0.5 M were added to 1 M Na-BP-DEGDME solution for making saturated state of Na metal. Concentration of saturated Na was measured as 1.1 M by inductively coupled plasma-optical emission analysis (ICP-OES). As a result, final chemical composition became saturated Na-1 M biphenyl-DEGDME. The anolyte is very sensitive to water and air. So that all of fabrication processes were done in glove box (less than O<sub>2</sub> ppm).

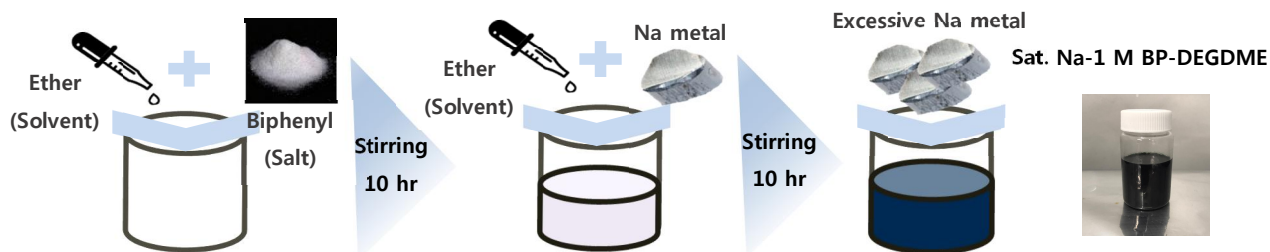


**Figure 22.** Fabrication process of saturated sodium-1 M biphenyl-DEGDME solution.

### 3.2. Chemical composition

To determine chemical composition of Na-BP, 3 components which are biphenyl, sodium and solvent, should be considered.

Firstly, appropriate salt concentration of electrolytes was studied. When salt concentration of is increasing up to about 1 M, conductivity is also increasing. However, too high concentration causes decreased mobility and conductivity. Appropriate concentration range is around 0.6 to 1.2 M. Therefore, biphenyl concentration is determined to 1 M (Fig. 23a).

Second is concentration of sodium. Electrochemical properties of various Na-BPs up to sodium concentration were tested in seawater coin cell. According to the results of power tests done in seawater battery coin cell with I-scan method (Scan rate:  $0.05 \text{ mA s}^{-1}$ ), saturated concentration of sodium indicates the highest power value as 8.2 mW. (Fig. 23b) The maximum power value of 1 M sodium concentration is about 7.2 mW. Reference anolyte is 1 M sodium triflate (NaTF) in TEGDME solvent and it shows 5.1 mW for maximum power value in same test condition.

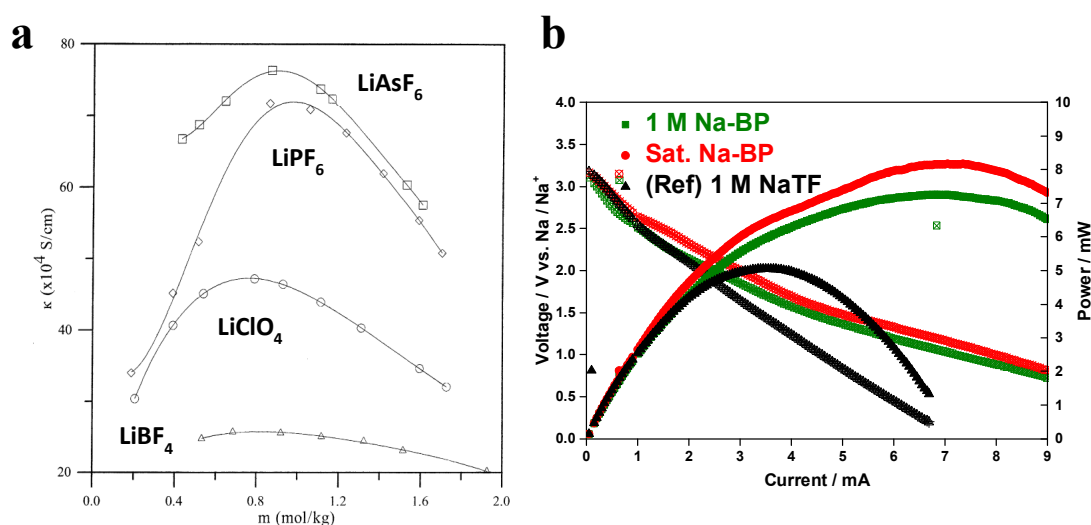


**Figure 23.** (a) Dependence of conductance on molality for PC 50.7%-DEC 49.3% per kinds of lithium-based salts <sup>24</sup>, (b) Power properties per sodium concentration of anolyte in seawater coin cell.

Last is kind of solvents. There are four kinds of representative glyme-based solvents. According to Table 1, DME solvent has too low boiling point so that if DME is used as solvent, it can be easily volatilized and hard to be fabricated with our cell sealing method. Therefore, I selected DEGDME solvent instead which has suitable boiling point and viscosity. Also, DEGDME has the highest donor number for ion dissociation.

Solvent	Molecular structure	$T_b$ [°C]	$\eta$ (cP) @25°C	DN
DME	<chem>COCOCCOC</chem>	84	0.46	18.6
DEGDME	<chem>COCOCCOCCOC</chem>	162	1.06	19.2
TEGDME	<chem>COC(CCOCCOC)CCOC</chem>	275	3.39	14

**Table 1.** Physicochemical properties of glyme-based solvents.

Moreover, when power tests were done in seawater battery coin cell with I-scan method (Scan rate:  $0.05 \text{ mA s}^{-1}$ ), Na-BP with DEGDME solvent shows the highest maximum power value as 8.2 mW (Fig. 24b). Otherwise, Na-BP with DME solvent shows 7.1 mW and TEGDME solvent shows 6.6 mW (Fig. 24a and 24c).

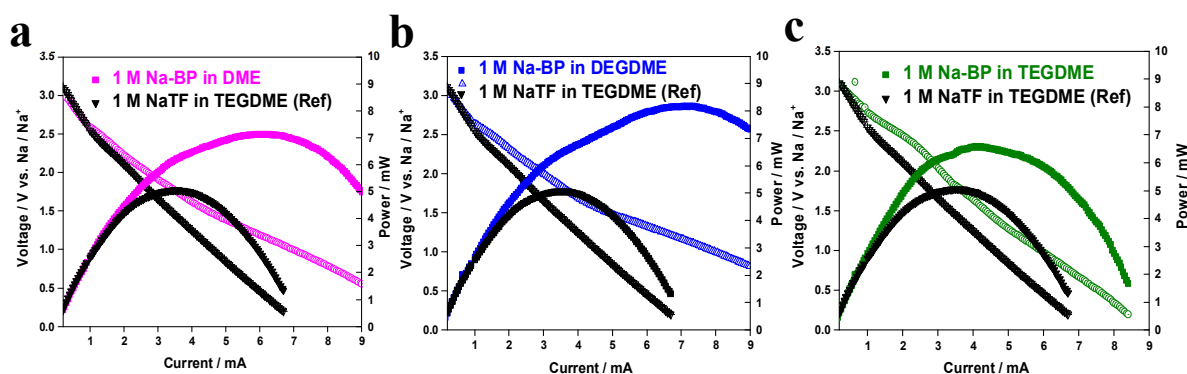


**Figure 24.** Power properties per kind of glyme-solvents of analyte in seawater coin cell; (a) 1,2-Dimethoxyethane (DME), (b) Diethylene glycol dimethyl ether (DEGDME), (c) Tetraethylene glycol dimethyl ether (TEGDME) (Reference analyte: 1 M NaTF-TEGDME).

### 3.3. Optimization of cell components

Sodium biphenyl (Na-BP) has highly reduceable properties. In that point, when Na-BP is applied in seawater battery, it causes leakage problems in sealing materials such as silicon glue ring. If silicon glues are immersed or contacted with Na-BP for the long times, glue would lose its adhesion properties and cause leakage and failure of the cell. For optimization of applying Na-BP in seawater coin cell, new sealants as alternative are found and they do not have any reactivity with Na-BP.

Also, to enhance ion affinity and wettability between Na-BP and separator, glass fiber which is optimized separator for Na-BP is used instead of conventional polyethylene separator.

Through these cell components, cycle life of the cell is highly increased and cell resistance is decreased.

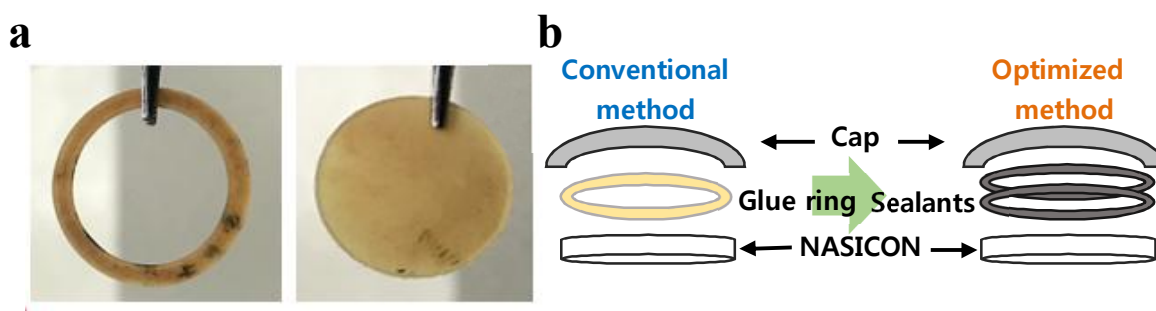


**Figure 25.** (a) Photographs of damaged silicon glues after immersed in Na-BP anolyte, (b) Conventional and optimized sealing method for seawater battery coin cell.

## 4. Conclusion

In summary, Alkali-biphenyl-ether solutions have been used as chemical prelithiation or presodiation agents or liquid anode in existing rechargeable battery systems. Among them, sodium-biphenyl-DEGDME (Na-BP) can be used as a liquid electrolyte by using the internal structural advantage that cathode and anode are physically separated due to NASICON solid membrane in seawater batteries.

In this study, it was confirmed that sodium biphenyl can sufficiently conduct Na ion as an alternative for existing organic electrolyte, sodium triflate-TEGDME (NaTF). In addition, it has high stability against Na metal anode which are commonly used in seawater batteries, so that decomposition reactions of electrolyte and anode which are the most serious problems of existing Na metal anode can be suppressed.

Through DEMS analysis, when Na-BP is used as an electrolyte, the generation of gas byproducts was insignificant and proved its effectiveness in a seawater pouch cells where these problems are prominent. Hereby, Na-BP can be sufficiently applied as an alternative electrolyte to solve the serious problems such as expansion of the cell, capacity decay in anode and depletion of the electrolyte.

In addition, since the decomposition reactions are suppressed and Na-BP does not form SEI layer between Na-BP and anode due to its electronic conductivity, it can have a homogenous interphase with the anode compared to the conventional electrolyte. Also, during Na plating process, it was confirmed that the size of plated Na grain with Na-BP electrolyte was sufficiently large and nucleation rate was retarded as much as 5 times than NaTF. We confirmed that the actual dendrite growth was inhibited by visual inspection through the Swagelok cell. Moreover, the results of Na-Na symmetric cell tests show Na-BP can reduce overpotential during cycling with improved cycle life of 10 times or more than NaTF.

Finally, Na-BP can have liquid anode properties as well with its intrinsic capacity and high reversibility. These properties were verified by constructing both liquid anode half-cell and seawater full-cell test. Furthermore, if Na-BP is applied as an electrolyte in seawater battery, it can compensate capacity of the existing anodes with its own capacity (Theoretical capacity:  $29.4 \text{ Ah L}^{-1}$ ,  $31.2 \text{ mAh g}^{-1}$ ). So, Na-BP can improve energy density of the cell with reliable reversibility.

As a conclusion, Na-BP has a 15 times lower price than that of existing electrolytes. Also, these research shows Na metal anode, which have been difficult to be commercialized due to gas evolution and unstable interfacial problems, could become a candidate of next-generation anode in large-scale battery systems.

## 5. References

- [1] World energy consumption by energy source (1990-2040), U. S. Energy Information Administration (EIA), *International Energy Outlook 2017*.
- [2] Total energy storage on grid (ESG) market, Installed capacity by region, World markets: 2012-2022, Pike Research, *Energy Storage Study Projects Boom Through 2022*.
- [3] Armaroli, N.; Balzani, V., Towards an electricity-powered world. *Energy & Environmental Science* **2011**, 4, 3193–3222.
- [4] Ragone plot comparing the performance of various batteries (energy density vs. output density), Atsusho Tsutsumi, *Fuel cell/battery system*.
- [5] Kim, Y.; Kim, H.; Park, S.; Seo, I.; Kim, Y., Na ion-Conducting Ceramic as Solid Electrolyte for Rechargeable Seawater Batteries. *Electrochimica Acta* **2016**, 191, 1-7.
- [6] Kim, Y.; Hwang, S. M.; Yu, H.; Kim, Y., High energy density rechargeable metal-free seawater batteries: a phosphorus/carbon composite as a promising anode material. *Journal of Materials Chemistry A* **2018**, 6, 3046-3054.
- [7] Han, J.; Hwang, S. M.; Go, W.; Senthilkumar, S. T.; Jeon, D.; Kim, Y., Development of Coin-Type Cell and Engineering of its Compartments for Rechargeable Seawater Batteries. *Journal of Power Sources* **2018**, 374, 24-30.
- [8] Kumai, K.; Miyashiro, H.; Kobayashi, Y.; Takei, K.; Ishikawa, R., Gas generation mechanism due to electrolyte decomposition in commercial lithium-ion cell. *Journal of Power Sources* **1999**, 81-82, 715–719.
- [9] Tao, R.; Bi, X.; Li S.; Yao, Y.; Wu, F.; Wang, Q.; Zhang, C.; Lu J., Kinetics Tuning the Electrochemistry of Lithium Dendrites Formation in Lithium Batteries through Electrolytes. *ACS Applied Materials & Interfaces* **2017**, 9, 7003–7008.
- [10] Medenbach, L.; Bender, C. L.; Haas, R.; Mogwitz, B.; Pompe, C.; Adelhelm, P.; Schroder, D.; Janek J., Origins of Dendrite Formation in Sodium–Oxygen Batteries and Possible

Countermeasures. *Energy Technology* **2017**, *5*, 2265 – 2274.

[11] Duan, H.; Yin, Y-X.; Shi, Y.; Wang, P-F.; Zhang, X-D.; Yang, C-P.; Shi, J-L.; Wen, R.; Guo, Y-G.; Wan, L-J., Dendrite-Free Li-Metal Battery Enabled by a Thin Asymmetric Solid Electrolyte with Engineered Layers. *Journal of the American Chemical Society* **2018**, *140*, 82-85.

[12] Yu, J.; Hu, Y-S.; Pan, F.; Zhang, Z.; Wang, Q.; Li, H.; Huang, X.; Chen, L., A class of liquid anode for rechargeable batteries with ultralong cycle life. *Nature communications* **2017**, *8*, 14629.

[13] Yu, X.; Pan, H.; Wan, W.; Ma, C.; Bai, J.; Meng, Q.; Ehrlich, S. N.; Hu, Y-S.; Yang X-Q., A Size-Dependent Sodium Storage Mechanism in  $\text{Li}_4\text{Ti}_5\text{O}_{12}$  Investigated by a Novel Characterization Technique Combining in Situ X-ray Diffraction and Chemical Sodiation. *Nano Letters* **2013**, *13*, 4721–4727.

[14] Chu, G.; Liu, B-N.; Luo, F.; Li, W-J.; Lu, H.; Chen, L-Q.; Li, H., Conductivity and applications of Li-biphenyl-1,2-dimethoxyethane solution for lithium ion batteries. *Chinese Physics B* **2017**, *26* (7), 78201.

[15] Westman, K.; Dugas, R.; Jankowski, P.; Wieczorek, W.; Gachot, G.; Morcretts, M.; Irisarri, E.; Ponrouch, A.; Palacin, M. R.; Tarascon, J.-M.; Johansson, P., Diglyme Based Electrolytes for Sodium-Ion Batteries. *ACS Applied Materials & Interfaces* **2018**, *1*, 2671-2680.

[16] Tan, K. S.; Yazami, R., Physical-Chemical and Electrochemical Studies of the Lithium Naphthalenide Anolyte. *Electrochimica Acta* **2015**, *180*, 629-635.

[17] Pan, F.; Yang, J.; Jia, C.; Li, H.; Wang, Q., Biphenyl-lithium-TEGDME solution as anolyte for high energy density non-aqueous redox flow lithium battery. *Journal of Energy Chemistry* **2018**, *27* (5), 1362-1368.

[18] Liang, F.; Qiu, X.; Zhang, Q.; Kang, Y.; Koo, A.; Hayashi, K.; Chen, K.; Xue, D.; Hui, K. N.; Yadegari, H.; Sun, X., A liquid anode for rechargeable sodium-air batteries with low voltage gap and high safety. *Nano Energy* **2018**, *49*, 574-579.

[19] Pan, H.; Lu, X.; Yu, X.; Hu, Y-S.; Li, H.; Yang, X-Q.; Chen, L., Sodium Storage and Transport Properties in Layered  $\text{Na}_2\text{Ti}_3\text{O}_7$  for Room-Temperature Sodium-Ion Batteries, *Advanced Energy Materials* **2013**, *3*, 1186-1194.

- [20] Liu, N.; Li, H.; Jiang, J.; Huang, X.; Chen, L., Li-Biphenyl-1,2-dimethoxyethane solution: Calculation and Its Application. *The Journal of Physical Chemistry B* **2006**, *110* (21), 10341-10347.
- [21] Park, S.; Senthilkumar, B.; Kim, K.; Hwnag, S. M.; Kim, Y., Saltwater as the energy source for low-cost, safe rechargeable batteries. *Journal of Materials Chemistry A* **2016**, *4*, 7207-7213.
- [22] Kim, D. H.; Choi, H.; Hwang, D. Y.; Park, J.; Kim, K. S.; Ahn, S.; Kim, Y.; Kwak, S. K.; Yu, Y.-J.; Kang, S. J., Reliable Seawater Battery Anode: Controlled Sodium Nucleation via Deactivation of Current Collector Surface. *Journal of Materials Chemistry A* **2018**, *6*, 19672-19680.
- [23] Huan, Y.; Wang, C.-Y.; Zuo, T.-T.; Wang, P.-F., Realizing a highly stable sodium battery with dendrite-free sodium metal composite anodes and O3-type cathodes. *Nano Energy* **2018**, *48*, 369-376.
- [24] Moumouzias, G.; Ritzoulis, G.; Siapakas, D.; Terzidis, D., Comparative study of LiBF<sub>4</sub>, LiAsF<sub>6</sub>, LiPF<sub>6</sub>, and LiClO<sub>4</sub> as electrolytes in propylene carbonate-diethyl carbonate solutions for Li/LiMn<sub>2</sub>O<sub>4</sub> cells. *Journal of Power Sources* **2003**, *122*, 57-66.
- [25] Yin, W.-W.; Fu, Z.-W., The Potential of Na-Air Batteries. *ChemCatChem* **2016**, *9*, 1545-1553.
- [26] Zhang, J.-G.; Wang, D.; Xu, W.; Xiao, Jie.; Williford, R.E., Ambient operation of Li/Air batteries, *Journal of Power Sources* **2010**, *194*, 4332-4337.
- [27] Aiken, C. P.; Xia, J.; Wang D. Y.; Stevens, D. A.; Trussier, S.; Dahn, J. R., An Apparatus for the Study of In Situ Gas Evolution in Li-Ion Pouch Cells. *Journal of the Electrochemical Society* **2014**, *161* (10), A1548-A1554.
- [28] Kim, J.-K.; Lee, E.; Kim, H.; Johnson, C.; Cho, J.; Kim, Y., Rechargeable Seawater Battery and Its Electrochemical Mechanism. *ChemElectroChem* **2014**, *2* (3), 328-332.
- [29] Kim, J.-K.; Mueller, F.; Kim, H.; Jeong, S.; Park, J.-S.; Passerini, S.; Kim, Y., Eco-friendly Energy Storage System: Seawater and ionic Liquid electrolyte. *ChemSusChem* **2016**, *9*, 42-49.



- [30] Kim, H.; Park, J-S.; Sahgong S. H.; Park, S.; Kim, J-K.; Kim, Y., Metal-free hybrid seawater fuel cell with an ether-based electrolyte. *Journal of Materials Chemistry A* **2014**, 2, 19584.
- [31] Kim, Y.; Kim, J-K.; Vaalma, C.; Bae, G. H.; Kim, G-T.; Passerini S.; Kim, Y., Optimized hard carbon derived from starch for rechargeable seawater batteries. *Carbon* **2018**, 129, 564-571.
- [32] Senthilkumar, S. T.; Bae, H.; Han, J.; Kim, Y., Enhancing Capacity Performance by Utilizing the Redox Chemistry of the electrolyte in a Dual-Electrolyte Sodium-Ion Battery. *Angewandte Chemie International Edition* **2018**, 57, 5335-5339.
- [33] Bommier, C.; Ji, X., Electrolytes, SEI formation, and Binders: A Review of Nonelectrode Factors for Sodium-Ion Battery Anodes. *Small* **2018**, 14, 1703576.
- [34] Tikekar, M. D.; Choudhury, S.; Tu, Z.; Archer, L. A., Design principles for electrolytes and interfaces for stable lithium-metal batteries. *Nature energy* **2016**, 1, 16114.
- [35] Kubota, K.; Komaba, S., Review – Practical Issues and Future Perspective for Na-Ion Batteries. *Journal of The Electrochemical Society* **2015**, 162 (14) A2538-2550.
- [36] Luo, Wei.; Shen, F.; Bommier, C.; Zhu, H.; Ji, X.; Hu, L., Na-Ion Battery Anodes: Materials and Electrochemistry. *Account of Chemical Research* **2016**, 49, 231-240.
- [37] Li, L.; Zheng, Y.; Zhang, S.; Yang, J.; Shao, Z.; Guo, Z., Recent progress on sodium ion batteries: potential high-performance anodes. *Energy & Environmental Science* **2018**, 11 (9), 2310-2340.
- [38] Kang, H.; Liu, Y.; Cao, K.; Zhao, Y.; Jiao, L.; Wang, Y.; Yuan, H., Update on anode materials for Na-ion batteries. *Journal of Materials Chemistry A* **2015**, 3 (35), 17899-17913.
- [39] Mertzger, M.; Strehle, B.; Solchenbach, S.; Gasteiger, H. A., Origin of H<sub>2</sub> Evolution in LIBs: H<sub>2</sub>O Reduction vs. Electrolyte Oxidation. *Journal of The Electrochemical Society* **2016**, 163 (5) A798-A809.
- [40] Siegel, J. B.; Stefanopoulou, A. G.; Hagans, P.; Ding, Yi.; Gorsich, D.; Expansion of Lithium Ion Pouch Cell Batteries: Observations from Neutron Imaging. *Journal of The Electrochemical*

*Society* **2013**, *160* (8) A1031-A1038.

[41] Ma, J.; Wang, C.; Wroblewski, S., Kinetic characteristics of mixed conductive electrodes for lithium ion batteries. *Journal of Power Sources* **2007**, *164* (2), 849-856.

[42] Tan, K. S.; Grimsdale, A.C.; Yazami R., Synthesis and Characterization of Biphenyl-Based Lithium Solvated Electro Solutions. *The Journal of Physical Chemistry B* **2012**, *116* (30), 9056-9060.